Sedimentary Geology 330 (2015) 1–15

Contents lists available at ScienceDirect

Sedimentary Geology

journal homepage: www.elsevier.com/locate/sedgeo

Mid-Late Pleistocene OSL chronology in western Amazonia and implications for the transcontinental Amazon pathway

Dilce F. Rossetti [a,*], Marcelo C.L. Cohen [b], Sonia H. Tatumi [c], André O. Sawakuchi [d], Édipo H. Cremon [a], Juan C.R. Mittani [c], Thiago C. Bertani [a], Casimiro J.A.S. Munita [e], Diego R.G. Tudela [f], Márcio Yee [c], Gabriela Moya [c]

[a] Instituto Nacional de Pesquisas Espaciais, São José dos Campos 12245970, SP, Brazil
[b] Universidade Federal do Pará, Belém 66075900, PA, Brazil
[c] Universidade Federal de São Paulo, Santos 11030400, SP, Brazil
[d] Universidade de São Paulo, Instituto de Geociências, São Paulo 05508080, SP, Brazil
[e] Instituto de Pesquisas Nucleares, São Paulo 05508900 SP, Brazil
[f] Universidade de São Paulo, São Paulo 05508900, SP, Brazil

ARTICLE INFO

Article history:
Received 12 August 2015
Received in revised form 30 September 2015
Accepted 1 October 2015
Available online 14 October 2015

Editor: Dr. B. Jones

Keywords:
OSL ages
Paleoenvironment
Fluvial systems
Mid-Late Pleistocene
Amazon reversal

ABSTRACT

The origin of the transcontinental Amazon drainage system remains unrevealed. Sedimentary deposits formed from the Neogene in the Amazonas and Solimões Basins constitute natural archives for reconstructing this event in space and time. However, paleoenvironmental and chronological analyses focusing on these deposits, or even their basic mapping, are still scarce to allow such investigation. In this context, primary interests are fluvial strata related to the lithostratigraphic Içá Formation, mapped over a widespread area in western Amazonian lowlands. Although long regarded as Plio-Pleistocene in age, this unit has not yet been dated and its overall depositional setting remains largely undescribed. The main goal of the present work is to contribute for improving facies analysis and chronology of these deposits, approaching an area in southwestern Amazonia and another in northern Amazonia, which are located more than 1000 km apart. Despite this great distance, the sedimentological and chronological characteristics of deposits from these two areas are analogous. Hence, facies analysis revealed paleoenvironments including active channel, abandoned channel, point bar, crevasse splay and floodplain, which are altogether compatible with meandering fluvial systems. Similarly, optically stimulated luminescence (OSL) dating revealed thirty three ages ranging from 65.4 ± 16.9 to 219.6 ± 25.1 ky (in addition to three outliners of 54.0 ± 7.6, 337.3 ± 36.9 and 346.6 ± 48.6 ky), and nine 97.1 ± 9.9 to 254.8 ± 23.8 ky for the areas in southwestern and northern Amazonia, respectively. These data lead to establish that deposits mapped as Içá Formation over a vast area of western Brazilian Amazonia have a Mid-Late Pleistocene age, rather than the previously inferred Plio-Pleistocene age. It follows that if Plio-Pleistocene deposits exist in this region they remain to be dated and must be restricted to a narrow belt in western Amazonia, as well as isolated occurrences underlying the Mid-Late Pleistocene strata characterized herein. The combination of data from this work with previously published provenance studies supports main Andean sediment sources only in the Mid-Late Pleistocene. It is proposed that before this time, the Amazon River was restricted to eastern Amazonia, being separated from western Amazonian drainage basins due to the presence of the Purus Arch. Erosion and/or subsidence of this geological feature would have promoted the connection of these drainage systems, ultimately with the expressive record of the transcontinental Amazon pathway into the Atlantic Ocean in the Mid-Late Pleistocene.

1. Introduction

The Amazon River constitutes the largest drainage basin on Earth, the majority developed over the Brazilian territory. This river is the longest of the planet, with about 6992 km in length (INPE, 2010), being responsible for delivering 20% of the world's freshwater into the Atlantic Ocean. It has over 1100 tributaries (Sterling, 1979), a water discharge of ~209,000 m^3/s, a drainage area of ~7,050,000 km^2, and a sedimentary load of 167 t/km^2 year. These characteristics guarantee its rank at the top list of megariver systems (Latrubesse, 2008).

Despite being the major drainage system on Earth, the origin of the Amazon River remains unclear. The most frequent interpretation is based on the assumption that this river had a primary westward flow that was diverted into a transcontinental eastward drainage. This was a response of the rise of the Andean Chain caused by the collision

* Corresponding author.
E-mail addresses: rossetti@dsr.inpe.br (D.F. Rossetti), mcohen80@hotmail.com (M.C.L. Cohen), sonia.tatumi@unifesp.br (S.H. Tatumi), andreos@usp.br (A.O. Sawakuchi), edipocremon@yahoo.com.br (É.H. Cremon), juanmittani603@hotmail.com (J.C.R. Mittani), thiagob@dsr.inpe.br (T.C. Bertani), camunita@net.ipen.br (C.J.A.S. Munita), diego_tudela@yahoo.com.br (D.R.G. Tudela).

http://dx.doi.org/10.1016/j.sedgeo.2015.10.001
0037-0738/

between the South American and Nazca plates. However, when the Amazon River flowed into the Atlantic Ocean as a transcontinental drainage has been an issue long under debate. A dispute has been about an old age in the Miocene at 14 Ma ago (Shepard et al., 2010) or around 6 Ma ago (e.g., Harris and Mix, 2002; Figueiredo et al., 2009; Mora et al., 2010), and an early Pliocene (Latrubesse et al., 2010) or even Pleistocene age (e.g., Bezerra, 2003; Horbe et al., 2013; Nogueira et al., 2013).

Fluvial deposits formed from the Neogene in the Amazonas and Solimões sedimentary basins witnessed the entire development of the Amazon drainage system, constituting natural archives that are invaluable for reconstructing its dynamic history in space and time. Despite this relevance, the sedimentologic, stratigraphic and chronologic analyses of these deposits are still deficient to approach this issue. In fact, there is an overall disagreement even on basic mapping of the various sedimentary units encompassing the Neogene–Holocene time-frame. Hence, the view has changed from the dominance of Neogene deposits over most of western Amazonia, represented by the Solimões Formation, to the prevalence of deposits related to the Içá Formation, presumably of Plio-Pleistocene age, over a vast (i.e., nearly 1,000,000 km^2) area of this region (e.g., Reis et al., 2006; CPRM, 2010). It has been also proposed that only 300,000 km^2 of western Amazonia were actually covered by the Içá Formation, with the remaining 700,000 km^2 being attributed to Late Pleistocene–Holocene deposits (Rossetti et al., 2005). Validating such proposal, which was based on remote sensing mapping integrated with a few ^{14}C ages, is a long-term task that will undoubtedly require a large volume of additional sedimentological information, as well as absolute dating analysis for providing a more robust chronology of the various sedimentary deposits existing over this region.

The aim of the present work is to contribute for improving facies analysis and the chronological framework of late Quaternary strata from the Amazonian lowland (Fig. 1A,B). Based on the analysis of pre-existing information combined with the data presented herein, a discussion is undertaken concerning the geographic and temporal distribution of these deposits and their implications for reconstructing the paleodynamics of the Amazon drainage basin, including the highly debated dispute about the time for the establishment of its eastward transcontinental connection to the Atlantic Ocean.

2. Study area and geological setting

Two study areas dominated by deposits referred as Içá Formation in geological maps (i.e., Reis et al., 2006; CPRM, 2010) were selected for this investigation. One is located at the margin of the Madeira River in southwestern Amazonia, between the city of Porto Velho and the town of Humaitá in the northern and southern States of Rondônia and Amazonas, respectively (Fig. 1C,D). The other area is located along a segment of the Branco River between the town of Caracaraí and its confluence with the Catrimani River (Fig. 1E), in the center-southern State of Roraima, northern Amazonia.

Despite the location in the Amazonian lowland, the study areas are under different climatic regimes. Hence, climate in southwestern Amazonia is tropical (Am in Köppen's classification), with a mean annual temperature of 28 °C and precipitation averaging 2500 to 3000 mm/year (Radambrasil, 1978); the latter has peaks in January to February, with the dry season between June and August. Climate in northern Amazonia is also tropical, but with a lower mean annual temperature of 24 °C and lower mean annual precipitation of 1500 mm yr^{-1} (Aw in Köppen's classification). In addition, the dry season is better defined than in other Amazonian areas, occurring from October to March, with a peak between December and March, when only 10% of the annual rainfall is received; the rainy season is between May and July. In this area, such peculiar climatic regime is modulated by seasonal shifts of the Intertropical Convergence Zone (ITCZ) and the El Niño Southern Oscillation (ENSO) (Latrubesse and Ramonell, 1994).

Geologically, the study areas are inserted in the center and northern portions of the Solimões Basin (Fig. 1B). The northern Solimões Basin is also referred as part of a separate structure reactivated in the Quaternary, namely *Pantanal Setentrional* (Santos et al., 1993; see also Rossetti et al., 2014a). The Solimões Basin encompasses ~600,000 km^2 and developed over igneous, metamorphic and volcanic sedimentary rocks of the Amazonian Craton (Tassinari and Macambira, 1999). This basin is separated from the Amazonas Basin to the east by the Purus arch, while the Iquitos arch makes its separation from the Acre Basin to the west. The northern and southern boundary of the Solimões Basin is the Guiana and Brazil Central shields, respectively (Fig. 1B). Primarily originated as an intracratonic rift during Early Paleozoic intraplate extension, this basin had a foreland stage due to deformation caused by the rise of the Andean Chain in the Cretaceous and Cenozoic. Sediment deposition, up to 3800 km thick, is initiated in the Proterozoic and continued in the Paleozoic, with reactivation in the Cretaceous and Cenozoic. Cenozoic deposits include the Miocene Solimões Formation, the Içá Formation of presumably Plio-Pleistocene age, as well as numerous unnamed Late Pleistocene–Holocene deposits which include, but are probably not exclusive of, fluvial terraces associated with the evolution of modern rivers (Rossetti et al., 2005).

The Solimões Formation consists of lacustrine to fluvio-deltaic deposits (e.g., Nogueira et al., 2013) and perhaps also transitional marine (e.g., Wesslingh et al., 2001) shales and sandstones. Originally regarded as Pliocene–Late Pleistocene or Late Pleistocene in age, these deposits were reinterpreted as Late Miocene (i.e., Huayquerian mammal age, 9–6.5 Ma; Cozzuol, 2006) or, more recently, Late Miocene to Pliocene (e.g., Latrubesse et al., 2010; Nogueira et al., 2013) in age.

The Içá Formation was originally defined as a reference to a succession of non-fossiliferous sandstones, subarkoses and secondarily mudrocks related to braided river systems exposed in western Amazonia, mainly along the Içá River (see h in Fig. 1), where its type-section is located (cf. Maia et al., 1977). Later, the geographic distribution of this unit was extended to encompass a much larger area (i.e., over 1,000,000 km^2) of the Amazonian lowland (e.g., Reis et al., 2006; CPRM, 2010; Fig. 1B), which resulted in its rank as the most widespread sedimentary unit exposed over this region. However, given the absence of fossils and highly oxidized nature, the Içá Formation was not dated yet, with its Plio-Pleistocene age being estimated with basis on its relative stratigraphic position overlying the Miocene–Pliocene Solimões Formation, and underlying Late Pleistocene–Holocene strata (Rossetti et al., 2005). These authors also documented the unconformable contacts of the Içá Formation with the underlying Solimões Formation and overlying Late Pleistocene–Holocene deposits.

3. Material and methods

The Içá Formation investigated here derives from several outcrops exposed along river banks and cores (see Fig. 1C–E for location). The latter were acquired using a RKS percussion drilling system, model COBRA mk1 (Eijkelkamp Agrisearch Equipment, Giesbeek, The Netherlands), which provided continuous cores 0.05 m in diameter at depths up to 15 m. The approach consisted on integrating facies, morphological and chronological data. The analysis of sedimentary facies included descriptions of characteristics such as lithology, texture, sedimentary structure and type of facies contact. Lateral variations in facies distribution were also annotated along river banks. The sedimentological features were properly photographed and recorded on measured lithostratigraphic profiles, which also provided the basis for selecting samples for dating.

Field data were plotted on a digital elevation model (DEM) derived from the Shuttle Radar Topography Mission—SRTM. Original 90-m resolution (i.e., 3 arc sec) synthetic aperture radar data acquired with C band ($\lambda = 6$ cm) and downloaded from the site http://edc.usgs.gov/srtm/data/obtainingdata.html was used in this study. SRTM data were processed using customized shades for correlating terrains with similar

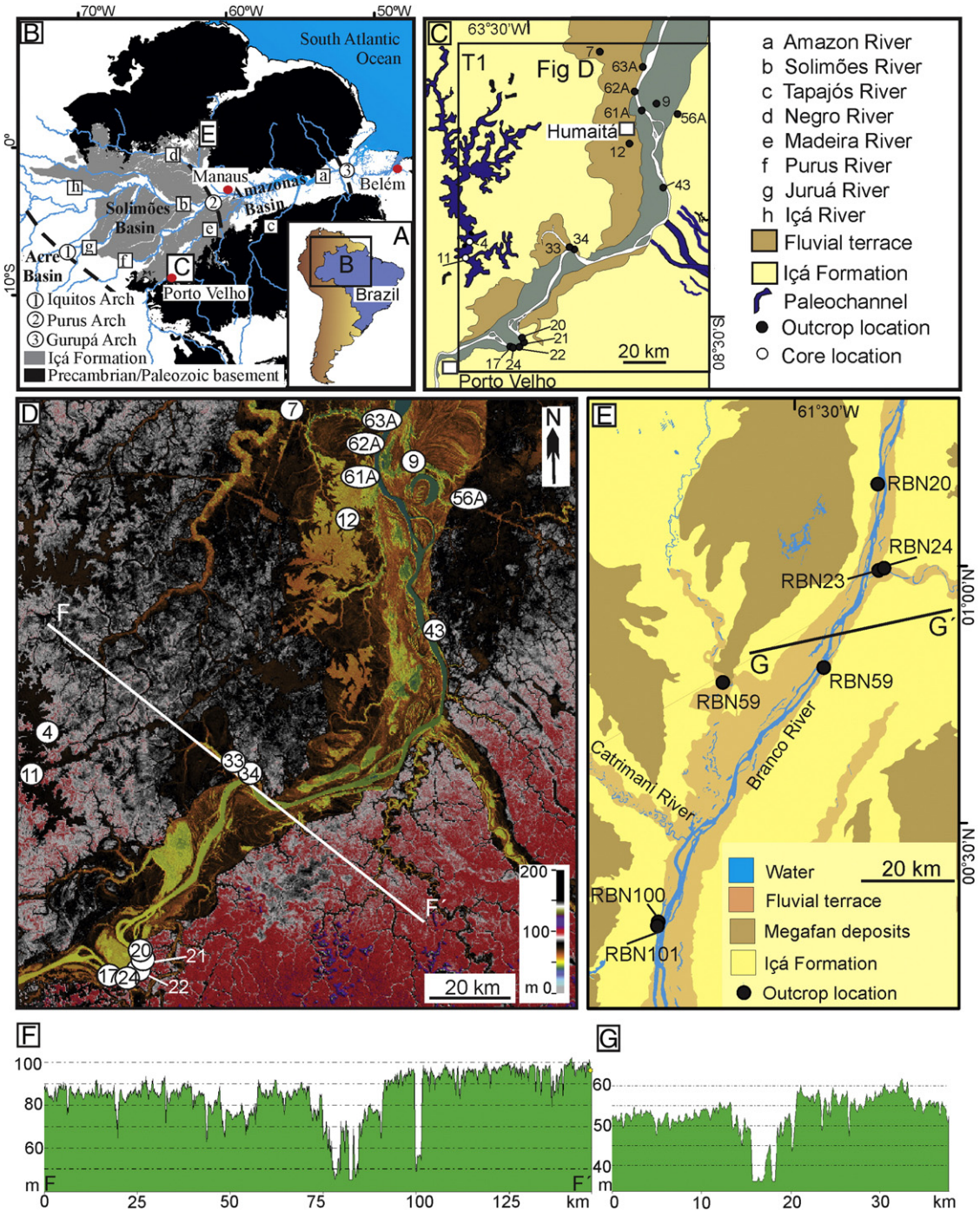

Fig. 1. Location map, as well as geological and geomorphological contexts of the studied areas in southwestern and northern of the Amazonian lowland. A) Location of the Amazonian lowland in northern Brazil. B) Location of the studied areas in the southern and northern parts of the Solimões Basin. This figure also locates the Purus and Iquitos arches, which separate this basin from the Acre and Amazonas basins to the west and east, respectively. In addition, distribution of the Içá Formation is shown in this figure (cf. Reis et al., 2006), which also includes the location of the Gurupá arch in the eastern margin of the Amazonas Basin. C) Geological context of the study area and of its neighborhood in southwestern Amazonian lowland, mostly between the city of Porto Velho and Humaitá, and location of the studies outcrops and cores (see figure B for location). D) DEM–SRTM of the study area in southwestern Amazonia lowland, illustrating the geomorphological context of the deposits mapped as Içá Formation, and as of the Madeira River terraces (see figure C for location). The transect F–F′ locates the topographic profile of figure F. E) Geomorphological context of the studied area in the northern Amazonian lowland, and location of the studied outcrops (see figure B for location; the trasect G–G′ locates the topographic profile of figure G). F,G) Topographic profiles extracted from the DEM–SRTM for the areas neighboring the Madeira and Branco Rivers in soutwestern and northern Amazonia, respectively. See location of F in C and of G in E.

morphological characteristics, which helped discriminating the studied deposits from other Quaternary strata present in the study areas.

To complete this study, facies-based field and remote sensing data were combined with laboratory studies applying Optically Stimulated Luminescence (OSL) of 45 sediment samples aiming to establish their chronology. Analyses were carried out at the Dating and Dosimetry Laboratory of the Federal University of São Paulo (UNIFESP) and the Luminescence and Gamma Spectrometry Laboratory (LEGaL) at University of São Paulo (USP-SP). OSL measurements were carried out in the Risø OSL/TL models DA-20 and DA-15 equipped with blue LEDs, Hoya U-340 filters and built-in $^{90}Sr/^{90}Y$ beta sources. Equivalent doses were determined through the single-aliquot regeneration (SAR) protocol as described in Murray and Wintle (2003) and Duller (2004). A dose recovery test was performed with given doses between 65 and

Table 1
Summary of radioisotope concentrations in samples dated by OSL. Potassium content in some samples are below detection limit (b.d.l.) of the used technique (Neutron Activation Analysis).

Sample	Coordinate lat/long	Depth m	U ppm	Th ppm	K %
PV4	7° 42′ 03.0″ S/63° 05′ 31.7″W	4.8	2.70 ± 0.22	10.5 ± 0.41	1.32 ± 0.11
PV4	7° 42′ 03.0″S/63° 05′ 31.7″W	6.3	1.93 ± 0.20	6.28 ± 0.20	0.52 ± 0.08
PV4	7° 42′ 03.0″S/63° 05′ 31.7″W	7.7	3.16 ± 0.44	8.12 ± 0.22	0.52 ± 0.08
PV7	7° 42′ 03.6″S/63° 10′ 10.1″W	7.2	3.17 ± 0.58	9.16 ± 0.55	1.19 ± 0.19
PV7	7° 42′ 03.6″S/63° 10′ 10.1″W	8.4	1.67 ± 0.56	7.53 ± 0.53	1.12 ± 0.26
PV9	7° 29′ 30.7″S/62° 55′ 42.7″W	6.3	3.65 ± 0.53	9.30 ± 0.82	1.15 ± O.04
PV9	7° 29′ 30.7″S/62° 55′ 42.7″W	7.3	1.88 ± 0.39	8.25 ± 0.50	1.10 ± 0.15
PV9	7° 29′ 30.7″S/62° 55′ 42.7″W	9.7	1.73 ± 0.40	7.48 ± 0.47	1.22 ± 0.19
PV9	7° 29′ 30.7″S/62° 55′ 42.7″W	12.3	0.64 ± 0.31	2.92 ± 0.38	0.56 ± 0.12
PV11	8° 09′ 25.6″ S/63° 47′14.9″W	6.8	1.21 ± 0.45	5.49 ± 0.37	0.67 ± 0.16
PV11	8° 09′ 25.6″ S/63° 47′14.9″W	7.5	1.45 ± 0.39	7.23 ± 0.46	1.51 ± 0.50
PV11	8° 09′ 25.6″ S/63° 47′14.9″W	8.9	2.02 ± 0.44	6.51 ± 0.43	0.84 ± 0.36
PV12	7° 37′ 38.5″ S/63° 04′87.0″W	5.6	3.20 ± 0.56	9.75 ± 0.60	1.55 ± 0.53
PV12	7° 37′ 38.5″ S/63° 04′87.0″W	6.8	1.84 ± 0.42	7.05 ± 0.43	1.1 ± 0.44
PV12	7° 37′ 38.5″ S/63° 04′87.0″W	7.7	1.95 ± 0.50	9.96 ± 0.61	1.16 ± 0.68
PV17	8° 37′ 08.6″ S/63° 34′42.8″W	2.8	3.13 ± 0.17	9.84 ± 0.35	1.13 ± 0.16
PV22	8° 36′ 38.6″ S/63° 32′ 46.5″W	2.8	6.14 ± 0.29	23.85 ± 0.85	b.d.l.
PV22	8° 36′ 38.6″ S/63° 32′ 46.5″W	7.8	6.49 ± 1.56	22.50 ± 0.81	b.d.l.
PV24	8° 13′21.2″ S/63° 16′21.3″W	9.0	2.24 ± 0.34	4.35 ± 0.40	b.d.l.
PV24	8° 13′21.2″ S/63° 16′21.3″W	11.0	1.44 ± 0.21	4.34 ± 0.16	0.01 ± 0.00
PV33	8° 09′32.6″ S/63° 19′16.9″W	3.20	2.21 ± 0.37	10.57 ± 0.60	1.09 ± 0.00
PV34	8° 09′59.8″ S/63° 18′44.0″W	12.2	1.82 ± 0.33	4.74 ± 0.28	0.88 ± 0.12
PV34	8° 09′59.8″ S/63° 18′44.0″W	13.3	1.14 ± 0.25	4.64 ± 0.28	0.99 ± 0.06
PV43	7° 51′ 12.2″ S/62° 53′ 49.3″W	2.0	1.01 ± 0.20	5.18 ± 0.31	0.35 ± 0.01
PV43	7° 51′ 12.2″ S/62° 53′ 49.3″W	8.0	1.4 ± 0.16	3.77 ± 0.14	0.63 ± 0.09
PV43	7° 51′ 12.2″ S/62° 53′ 49.3″W	10.1	1.01 ± 0.17	4.74 ± 0.14	0.042 ± 0.01
PV43	7° 51′ 12.2″ S/62° 53′ 49.3″W	12.7	1.42 ± 0.39	4.34 ± 0.16	b.d.l.
PV56A	7° 33′ 39.7″ S/62° 50′ 09.1″W	2.2	2.48 ± 0.00	13.06 ± 0.00	0.506 ± 0.03
PV56A	7° 33′ 39.7″ S/62° 50′ 09.1″W	3.4	1.19 ± 0.00	5.71 ± 0.00	0.258 ± 0.02
PV61A1	7° 29′ 51.7″ S/63° 01′ 17.5″W	7.9	1.81 ± 0.00	7.78 ± 0.00	0.592 ± 0.03
PV61A1	7° 29′ 51.7″ S/63° 01′ 17.5″W	17.2	1.02 ± 0.00	2.45 ± 0.00	0.127 ± 0.01
PV62A1	7° 26′ 15.4″ S/63° 01′ 10.9″W	7.2	1.82 ± 0.00	7.67 ± 0.00	0.661 ± 0.03
PV62A2	7° 26′ 15.4″ S/63° 01′ 10.9″W	12.3	1.59 ± 0.00	7.22 ± 0.00	0.598 ± 0.03
PV62A2	7° 26′ 15.4″ S/63° 01′ 10.9″W	14.1	2.34 ± 0.00	11.17 ± 0.00	0.609 ± 0.03
PV63A	7° 23′ 01.0″ S/62° 59′ 50.0″W	13.2	1.08 ± 0.00	4.79 ± 0.00	0.640 ± 0.03
PV63A	7° 23′ 01.0″ S/62° 59′ 50.0″W	16.7	1.21 ± 0.00	4.69 ± 0.00	0.725 ± 0.04
RBN20	1° 09′ 34.2″ N/61° 20′18.6″W	1.8	1.07 ± 0.00	4.06 ± 0.00	0.07 ± 0.01
RBN20	1° 09′ 34.2″ N/61° 20′18.6″W	2.0	0.90 ± 0.00	4.02 ± 0.00	0.04 ± 0.01
RBN23	0° 39′ 31.6″ N/61° 19′55.1″W	4.0	1.97 ± 0.00	10.52 ± 0.00	0.20 ± 0.02
RBN23	0° 39′ 31.6″ N/61° 19′55.1″W	4.9	1.91 ± 0.00	10.29 ± 0.00	0.20 ± 0.02
RBN24	0° 59′ 43.3″ N/61° 19′36.6″W	1.9	1.14 ± 0.00	2.68 ± 0.00	0.06 ± 0.01
RBN59	0° 46′ 23.9″ N/61° 38′25.3″W	1.4	0.67 ± 0.00	0.95 ± 0.00	0.04 ± 0.01
RBN100	0° 18′ 18.1″ N/61° 45′59.5″W	6.9	1.65 ± 0.00	7.34 ± 0.00	0.12 ± 0.01
RBN101	0° 18′ 27.6″ N/61° 45′56.4″W	4.7	1.75 ± 0.00	7.08 ± 0.00	0.11 ± 0.01
RBN103	0° 48′ 07.8″ N/61° 26′28.3″W	6.9	1.25 ± 0.00	4.92 ± 0.00	0.07 ± 0.01

b.d.l. = below detection level.

175 Gy. Only aliquots with recycling ratio between 0.9 and 1.1, recuperation less than 5% and negligible infrared stimulation signal were used for equivalent dose calculation. Concentrations of natural radionuclides for dose rate calculation were determined with high resolution gamma spectrometry using a high purity germanium detector (relative efficiency of 55%) in an ultralow background shield. The activities of ^{40}K and ^{238}U and ^{232}Th daughter nuclides were calculated through an efficiency calibration based on ISOCS (In Situ Object Counting System) for the used HPGe detector. The radioactive isotope contents of part of the samples were also determined by Genie-2000 instrumental neutron activation analysis (INAA) using a Canberra S-100 MCA detector with 8192 channels. Samples were irradiated in the research reactor's pool IAE-R1 at the Institute of Nuclear Research (IPEN-CNEN), Brazil. Constituent elements in coal fly ash (NIST-SRM-1633b) and trace elements in soil (IAEA-Soil 7) were used as a standard and to check the analysis, respectively. Radionuclide concentrations were converted in dose rates using conversion factors by Adamiec and Aitken (1998) and Guérin et al. (2011) considering attenuation by water saturation. The cosmic dose rate was calculated through the sample's latitude, longitude, elevation, burial depth and density (Prescott and Stephan, 1982). The total error of the dose rate and ages was calculated according the Gaussian law of error propagation. In average, 14 aliquots per sample were analyzed, with exponential or linear–exponential growth functions being used to describe dose–response curves. Equivalent doses were calculated using the central age model (CAM) (Galbraith et al., 1999). The central age model (CAM) and minimum age model (MAM) were used for over-dispersion lower or greater than 0.30, respectively.

The new data acquired in this study were combined with information from pre-existing publications focusing on sediment provenance in order to provide the basis for discussing the establishment of the Amazon River.

4. Chronology and general morphological context

The studied deposits assigned to the Içá Formation in geological maps form continuous terrains distributed along both sides of the Madeira (Fig. 1C,D) and Branco Rivers (Fig. 1E) in southwestern and northern Amazonia, respectively. In southwestern Amazonia, these deposits are topographically higher at the right margin of the Madeira River, where most of the altitudes range from 95 to 100 m (Fig. 1F). Northward in this side of the river and also in its left margin, the Içá Formation occurs in terrains with slightly lower altitudes ranging from 80 to 90 m. These deposits were included as part of terrace 1 in Rossetti et al. (2014b), who reported ^{14}C ages older than ~43 ka. In the present

work, dating of quartz grains from sandstones belonging to these strata provided thirty three OSL ages within the range of 65.4 ± 16.9 to 219.6 ± 25.1 ky, with three younger outliners of 54.0 ± 7.7 ky (PV11) and two older outliners of 337.3 ± 36.9 (PV24) and 346.6 ± 48.6 ky (PV43) (Tables 1 and 2; Figs. 2A, 3, 4A). It is interesting to note that, except to one instance (PV11), all other profiles showed consistent age distribution, with an expected upward decrease in values. The only exception occurred in PV11, where an oldest age (i.e., 126.9 ± 15.5 ky) was achieved at a shallower depth relative to a younger age (i.e., 101.9 ± 23.6 ky) below. However, this result was also considered good, as it points to nearly similar ages considering the indicated errors. It is important to highlight that the oldest samples presented equivalent doses near reliable maximum doses ($2D_0$) that can be estimated for quartz using the blue stimulation OSL signal.

A remarkable feature to the left of the Madeira River is an elongated dendritic paleomorphology related to an ancient southward flowing drainage cut down into the Içá Formation, and which became abandoned through time converting into a fluvial ria (Bertani et al., 2014). According to these authors, mudstones from drills acquired through these features recorded AMS ages ranging from 5928–6124 to 21,547–22,285 cal yrs BP from the uppermost 5.5 m depth. In the present work, six older ages between 54.0 ± 7.6 and 126.9 ± 15.5 ky were obtained for sandstones below this depth (see PV4 and PV11 in Table 2 and Fig. 6).

In northern Amazonia, the deposits related to the Içá Formation occur also on both sides of the Branco River, where they are positioned topographically lower than in southwestern Amazonia, i.e., usually at altitudes <60 m (Fig. 1G). However, recent publications (i.e., Rossetti et al., 2012, 2014a) showed that at least great part of the deposits previously mapped as Içá Formation in this area records a Late Pleistocene–Holocene sandy sedimentation originated by distributary drainage networks of megafan depositional systems. The development of such drainage systems would have produced well-defined triangular-shaped paleomorphologies up to several kilometers in length over older alluvial deposits related to the Içá Formation. OSL dating of the latter deposits that occur external to the megafans resulted in nine ages ranging from 102.1 ± 9.0 to 245.8 ± 23.8 ky (Table 1; Fig. 7A).

Table 2
OSL dated samples with corresponding depths, equivalent doses (De), recycling (RC) and recuperation (RP) rates, annual dose rates due to cosmic radiation ($AD_{c.r.}$), total annual dose rate (AD) and OSL ages.

Sample	Depth (m)	RC rate	RP rate	$AD_{c.r.}$ (Gy/ky)	De (Gy)	AD (Gy/ky)	Age (ky)
PV4	4.8	1.020	0.330	0.10	213 ± 28	3.94 ± 2.25	54.0 ± 7.6
PV4	6.3	0.970	0.250	0.06	184 ± 16	2.17 ± 0.94	84.9 ± 8.3
PV4	7.7	1.050	0.200	0.09	259 ± 34	2.77 ± 1.00	93.5 ± 12.7
PV7	7.2	1.040	0.138	0.07	124 ± 20	1.78 ± 0.14	69.6 ± 12.6
PV7	8.4	1.030	0.166	0.06	130 ± 12	1.39 ± 0.16	99.3 ± 14.5
PV9	6.3	0.981	0.239	0.07	81 ± 21	2.02 ± 0.01	40.3 ± 15.0
PV9	7.3	0.983	0.237	0.06	107 ± 18	1.49 ± 0.11	72.1 ± 12.9
PV9	9.7	0.980	0.253	0.05	117 ± 16	1.48 ± 0.12	79.0 ± 12.7
PV9	12.3	0.985	0.238	0.04	94 ± 19	0.63 ± 0.08	148 ± 34.8
PV11	6.8	1.020	0.166	0.07	162 ± 05	1.27 ± 0.15	126.9 ± 15.5
PV11	7.5	0.983	0.257	0.06	170 ± 26	1.66 ± 0.29	101.9 ± 23.6
PV11	8.9	0.985	0.237	0.05	154 ± 25	1.26 ± 0.21	122.3 ± 28.4
PV12	5.6	0.973	0.106	0.08	154 ± 33	2.36 ± 0.35	65.4 ± 16.9
PV12	6.8	1.040	0.100	0.07	146 ± 18	1.57 ± 0.28	92.9 ± 20.2
PV12	7.7	1.010	0.098	0.06	195 ± 19	1.64 ± 0.39	118.9 ± 30.7
PV17	2.8	1.010	0.260	0.13	263 ± 19	2.42 ± 0.13	108.4 ± 9.6
PV22	2.8	0.990	0.360	0.13	285 ± 29	2.90 ± 0.07	98.2 ± 10.3
PV22	7.8	0.980	0.370	0.06	266 ± 18	2.69 ± 0.24	98.8 ± 11.1
PV24	9.0	0.915	0.114	0.17	141 ± 28	0.93 ± 0.07	151 ± 32.5
PV24	11.0	1.010	0.240	0.05	215 ± 20	0.64 ± 0.04	337.3 ± 36.9
PV33	3.20	0.990	0.220	0.12	131 ± 11	1.69 ± 0.08	77.8 ± 7.2
PV34	12.2	0.992	0.117	0.03	113 ± 20	1.14 ± 0.09	99.4 ± 19.6
PV34	13.3	0.984	0.114	0.03	118 ± 22	1.10 ± 0.06	108.0 ± 20.4
PV43	2.0	0.988	0.075	0.14	111 ± 02	0.78 ± 0.04	142.0 ± 7.6
PV43	8.0	1.040	0.200	0.06	232 ± 20	1.17 ± 0.07	198.7 ± 21.3
PV43	10.1	0.995	0.226	0.05	147 ± 27	0.74 ± 0.04	197.8 ± 37.3
PV43	12.7	1.020	0.300	0.03	213 ± 19	0.62 ± 0.06	346.6 ± 48.6
PV56A	2.2	1.005	0.145	0.14	200 ± 26	1.95 ± 0.14	102.8 ± 15.2
PV56A	3.4	0.999	0.147	0.13	200 ± 22	1.03 ± 0.07	190.2 ± 25.4
PV61A1	7.9	1.003	0.147	0.13	156 ± 10	1.61 ± 0.13	97.1 ± 9.9
PV61A1	17.2	1.024	0.403	0.13	127 ± 11	0.58 ± 0.04	219.6 ± 25.1
PV62A1	7.2	0.995	0.250	0.10	175 ± 14	1.71 ± 0.14	102.3 ± 11.6
PV62A2	12.3	1.003	0.163	0.07	169 ± 14	1.47 ± 0.11	115.1 ± 13.0
PV62A2	14.1	1.009	0.250	0.07	185 ± 19	2.00 ± 0.16	92.4 ± 12.1
PV63A	13.2	1.014	0.136	0.07	152 ± 09	1.25 ± 0.10	121.4 ± 12.2
PV63A	16.7	0.993	0.107	0.06	190 ± 20	1.28 ± 0.10	148.2 ± 19.1
RBN20	1.8	0.993	0.145	0.15	129 ± 10	0.76 ± 0.05	169.5 ± 17.4
RBN20	2.0	1.000	0.022	0.16	120 ± 07	0.69 ± 0.05	175.0 ± 15.0
RBN23	4.0	0.985	0.120	0.15	142 ± 08	1.39 ± 0.10	102.1 ± 9.0
RBN23	4.9	0.994	0.020	0.14	146 ± 07	1.40 ± 0.10	104.7 ± 8.7
RBN24	1.9	0.962	0.177	0.15	127 ± 07	0.66 ± 0.04	192.6 ± 16.0
RBN59	1.4	1.004	0.103	0.14	97 ± 08	0.40 ± 0.02	254.8 ± 23.8
RBN100	6.9	0.983	0.297	0.11	146 ± 14	1.06 ± 0.01	137.6 ± 13.3
RBN101	4.7	1.053	0.299	0.12	158 ± 10	1.10 ± 0.01	143.1 ± 9.5
RBN103	6.9	1.025	0.100	0.13	173 ± 11	0.75 ± 0.01	231.1 ± 1.8

5. Sedimentological description

As shown above, deposits assigned to the Içá Formation in both study areas display concurring Mid-Late Pleistocene OSL ages, despite their location more than 1000 km apart. Their sedimentological characteristics are also comparable, being dominated essentially by fine- to coarse-grained sandstones generally interbedded with mudstone; heterolithic deposits and conglomerates are locally present, although secondarily. The deposits display high degree of oxidation. Iron oxides and hydroxides are locally concentrated in porous sandy layers, forming highly ferruginous and indurated beds (e.g., see Fe in profiles PV17 and PV21 in Figs. 2, 4 and 5 and in profile RBN 20 in Fig. 7A, B). Iron oxides/hydroxides are also present in these deposits as dispersed ferruginous concretions, particularly in the Roraima profiles, where incipient lateritic paleosols are present at their tops (e.g., see Fig. 7A and Lp in Fig. 7C,D). This process of soil formation was in part responsible for the dominantly massive nature of the studied deposits. However, several sedimentary structures are present lower in the sections, which favored approaching the depositional processes and environments. Hence, the sedimentological analysis led to recognize five depositional environments attributed to active channel, abandoned channel, channel bar, floodplain and crevasse splay. These were related to fluvial depositional systems, as described in the following.

Active channel deposits are the most representative of the studied areas, occurring in all sections (see Figs. 2–7). They consist of packages up to 12 m thick of poorly-sorted, either massive or stratified-sandstones that chiefly vary in grain size from medium- to very-coarse, although fine-grained and pebbly sandstones are also present. The stratified-sandstones are dominated by medium-scale, either planar or trough cross stratifications and, less frequently, parallel and trough cross laminations (Figs. 2B, 5A–D, 7B,D). Sandstones may grade downward into massive or stratified-conglomerate formed mostly by pebbles (usually <5 cm in diameter) of quartz and lithic (i.e., sedimentary and metamorphic rocks) compositions. Conglomerates of quartz pebbles and clasts of ferruginous concretions are locally present at one locality (see profile PV17 in Fig. 2A). This facies has matrix consisting of invariably fine- to coarse-grained quartz-sandstones. The conglomerates are massive or display medium- or large-scale cross stratification and they typically grade upward into sandstones, forming fining- and thinning-upward successions (Figs. 2A, 5A–C, 6, 7A,B,E). A remarkable feature of these successions is their lower undulatory, locally concave up-shaped, basal bounding surfaces with erosional reliefs of several meters at the outcrop scale.

Abandoned channel deposits are the second most frequent facies association of the study area, where they reach up to 6 m thick. They consist of muddy successions that grade downward into active channel deposits to complete fining-upward successions. The abandoned

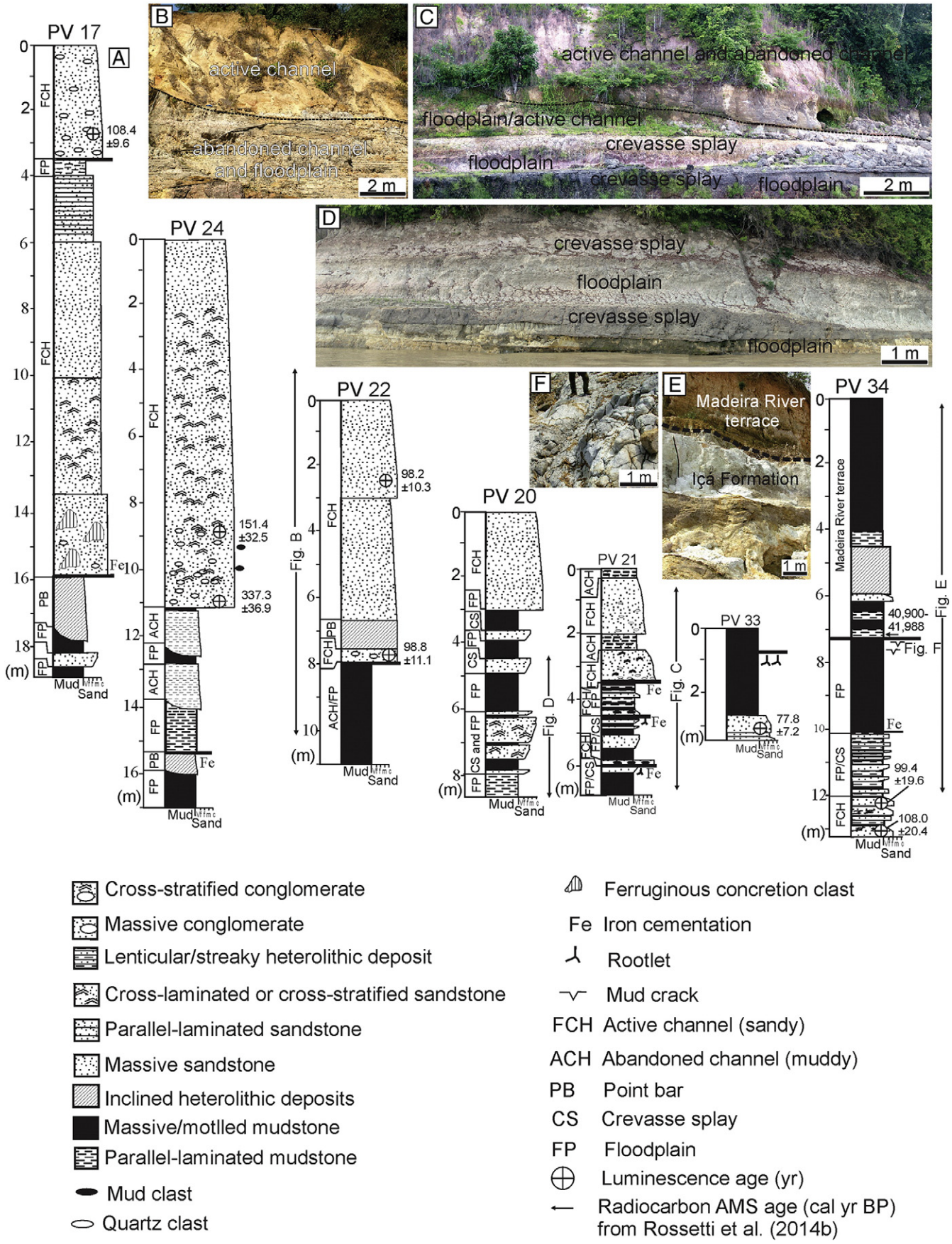

Fig. 2. Sedimentological data of the study area in southwestern Amazonia (see location in Fig. 1). A) Lithostratigraphic profiles PV17, PV24, PV 22, PV20, PV21 and PV 34 with location of the OSL ages. Radiocarbon AMS age shown in PV34 is from Rossetti et al. (2014b). B–D) Views of sedimentary deposits in profiles PV24 (B), PV 21 (C), PV 20 (D) and PV 34 (E) (see location of these details in A). F) Detail of E, illustrating mud cracks over the unconformity at the top of the Içá Formation.

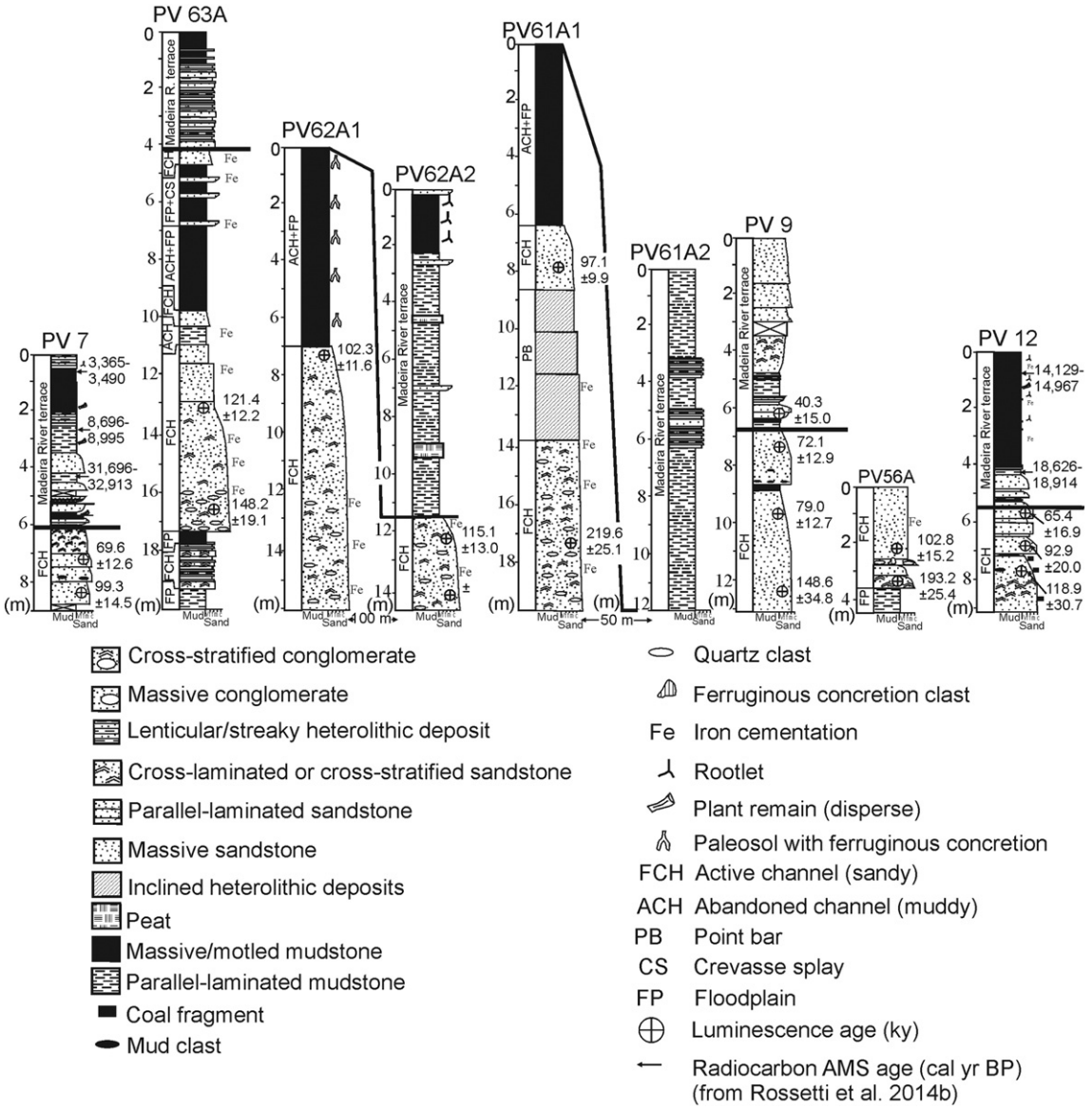

Fig. 3. Sedimentological data of the study area in southwestern Amazonia (see location in Fig. 1) with OSL ages. Radiocarbon AMS ages in profiles PV7 and PV12 are from Bertani et al. (2014) and Rossetti et al. (2014b).

channel deposits can also occur as isolated packages confined to concave-up basal bounding surfaces that cut down into floodplain deposits. Mudstones from abandoned channels vary from parallel-laminated to massive/mottled or heterolithic deposits. The latter are mostly of streaky or lenticular types and contain sandy components that are either massive or trough cross-laminated. Heterolithic and parallel-laminated mudstones occur isolated or grade upward into massive mudstone (e.g., PV4, PV11 in Fig. 6 and PV43 in Fig. 5), which locally display root marks.

Channel bar deposits are locally present, being recorded solely in profiles PV17, PV22 and PV24 in southwestern Amazonia (Fig. 2A). These deposits reach up to 2 m thick and they are typified by low-angle (i.e., $<15^0$), inclined beds formed by alternations of sandstones and mudstones. Sandstones are moderately to well sorted, fine- to medium-grained. They form beds 0.2–0.3 m thick that are separated by reactivation surfaces mantled by thin mudstone layers. Sandstones are internally massive or they display mostly planar, small-scale cross stratification or cross lamination.

Floodplain deposits are compositionally similar to abandoned channel deposits, being also composed of parallel-laminated mudstone, massive/mottled mudstone and/or heterolithic deposits (Figs. 2, 4, 7A,C). However, they were differentiated based on their tabular geometry and lateral continuity along river banks. Additionally, they are more frequently thinner (i.e., <2 m thick) and generally alternate with crevasse splay deposits (see descriptions below). Root marks and mud cracks were recorded in the floodplain deposits.

Crevasse splay deposits are composed by moderate to well sorted, silty- to fine-grained sandstones up to 1 m thick that are interbedded with floodplain deposits. At the outcrop scale, crevasse splay deposits are characterized by laterally discontinuous bodies up to several meters in length, which occur either isolated or as amalgamated sand bodies within floodplain mudstones (profiles PV 20 and 21 in Fig. 1A; Fig. 1C,D; profile RBN23 in Fig. 7A,C). The geometry of crevasse splay deposits varies from lobate to wedge-shaped. These sandstones are massive, parallel- or trough or planar cross-laminated (see Fig. 1D), as well as climbing cross-laminated. In addition to the lenticular geometry, the most striking characteristic that allowed discriminate these deposits from other sandy deposits in the studied areas was their organization into coarsening-upward successions that grade downward into floodplain deposits. The top of

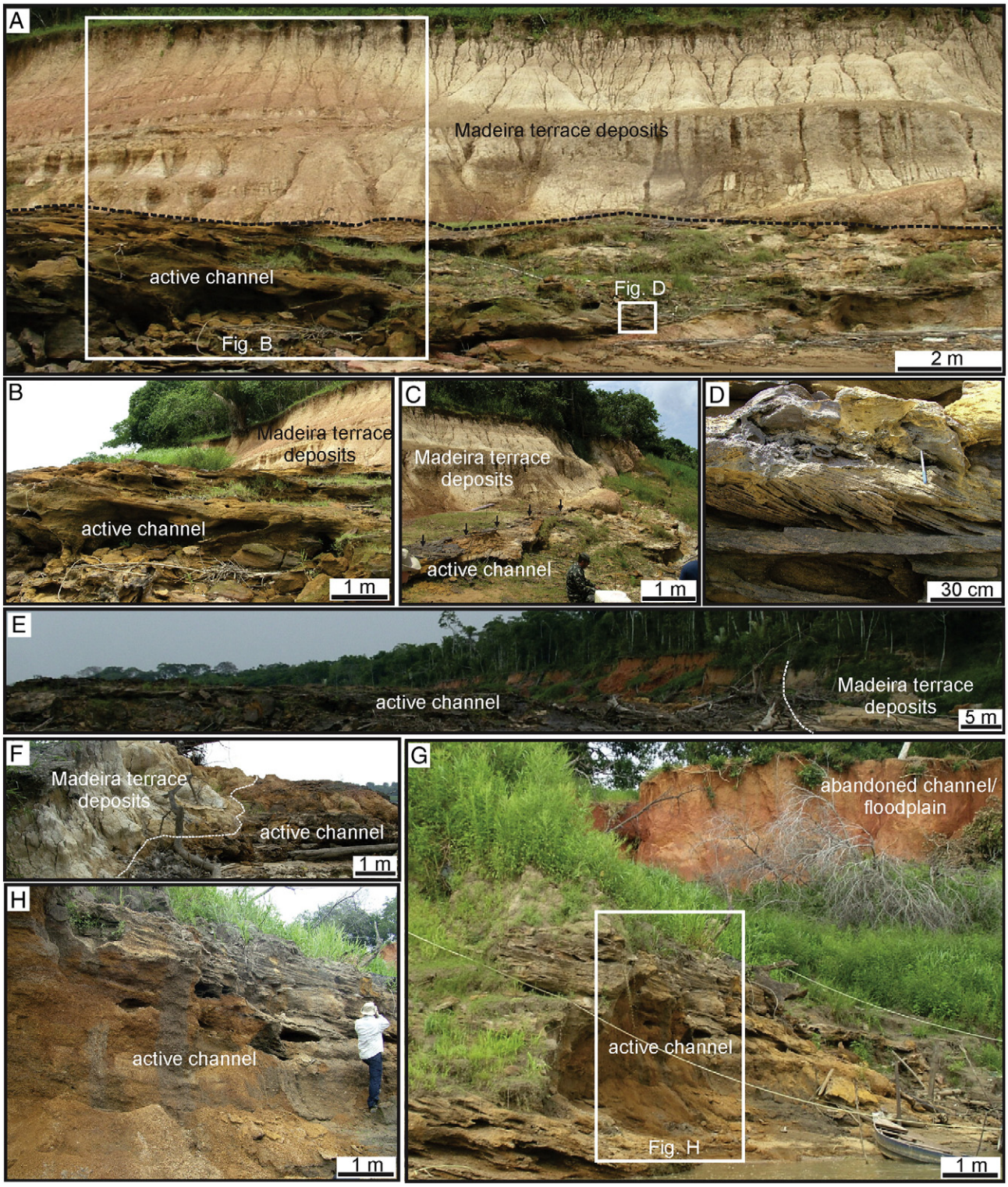

Fig. 4. View of sedimentary deposits in profiles PV63A, PV62A and PV61A shown in Fig. 3. A) General view of outcrop in PV63A, illustrating active channel deposits overlain by deposits of the Madeira terrace. The dashed line indicates the unconformity between these units. B) Detail of sandstone from the active channel deposits shown in A. C) Detail of the unconformity shown in A, which is marked by ferruginous cementation (indicated by the set of black arrows). D) Detail of cross-stratified sandstones from active channel deposits (see figure A for location). E,F) General view (E) and detail (F) of outcrop in PV62A with active channel sandstones in sharp contact with deposits of the Madeira terrace. G,H) General view (G) and (H) detail of outcrop in PV61A illustrating active channel deposits overlain by abandoned channel/floodplain deposits (see location of H in G).

the crevasse splay deposits are essentially sharp and may display root marks.

At some localities, the studied deposits are unconformably overlain by younger strata representative of the Madeira River terraces (Figs. 3, 6, 7A–C, E, F, see also PV34 in Fig. 2).

6. Paleoenvironmental analysis and type of depositional system

The set of deposits described above characterizes fluvial depositional systems over the entire studied areas. This is particularly shown by the great incidence of deposits formed by confined flows within active and

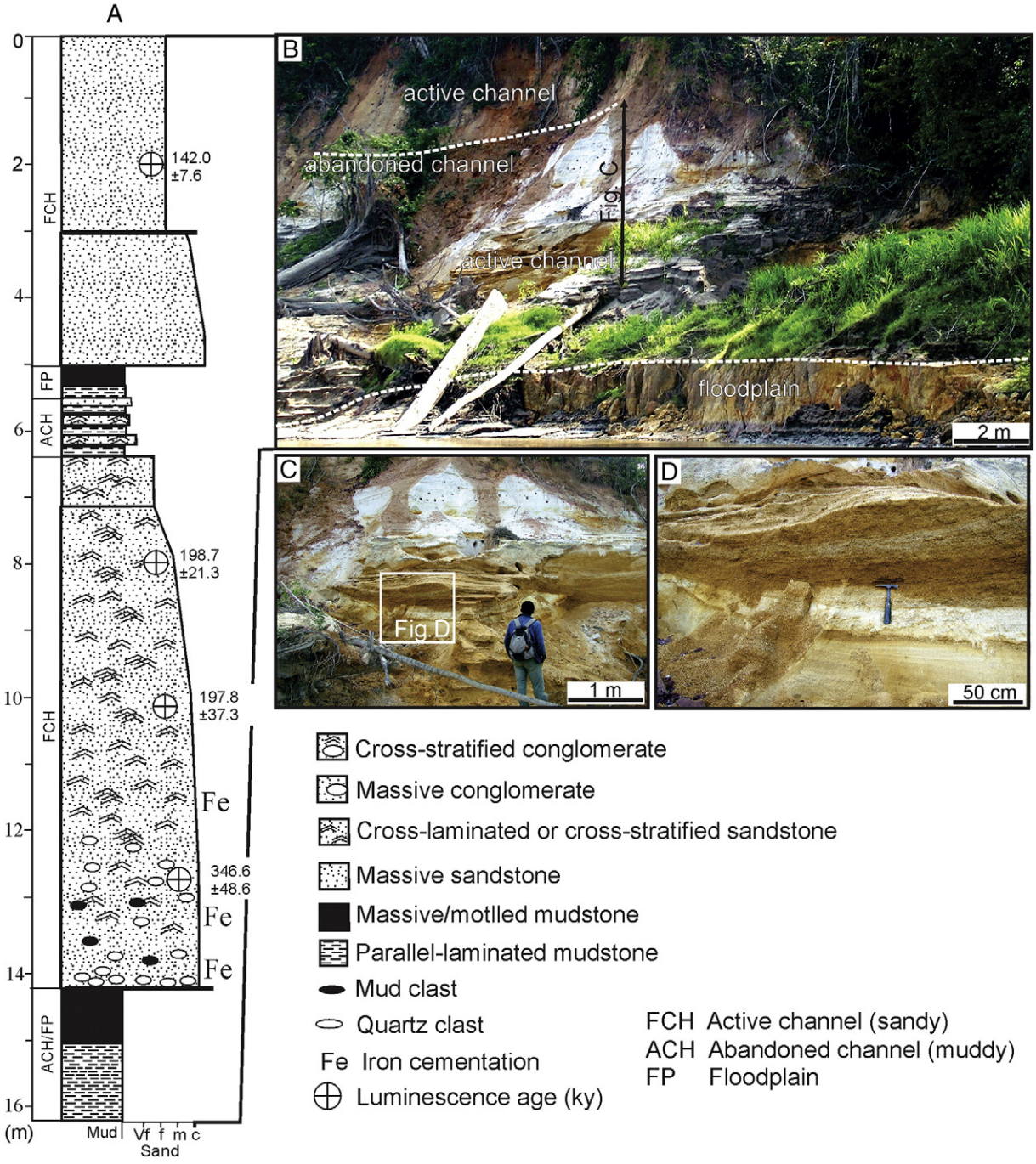

Fig. 5. Sedimentological data of the study area in southwestern Amazonia (see location in Fig. 1). A) Lithostratigraphic profile PV43, with location of the OSL ages obtained in this work. B) General view of the outcrop, with the spatial distribution of floodplain, active channel and abandoned channel deposits (white dashed lines bound deposits representative of depositional environments). C,D) Details of the trough cross-stratified sandstones from active channel deposits (see location of figures C and D in figures B and C, respectively).

abandoned channel environments, as indicated by the high frequency of thinning- and fining-upward sedimentary successions bounded by sharp, erosional, and commonly scoop-shaped, basal discontinuities. Such characteristics, related to decreasing flow energy through time, are typical of many documented channel deposits (e.g., McLaurin and Steel, 2007). High energy, bedload sedimentation is recorded at the base of these channels by fine- to coarse-grained sandstones and conglomerates having planar or trough cross stratification formed respectively by migration of small- to medium-scale 2-D or 3-D bedforms under unidirectional low flow regime. Large-scale and low-angle dipping sandstone/mudstone interbeddings within these channels are attributed to the record of mixed-load channel bars, probably point bars. Channels with conglomerates constituted by clasts of ferruginous concretions suggest scouring of pre-existing lateritic palosols, probably eroded from the unconformity at the top of the underlying Solimões Formation, where these paleosols are well documented (e.g., Rossetti et al., 2005). The frequent upward gradation from sandy to muddy channel deposits attests channel abandonment as a recurrent process throughout the study areas. As channels became abandoned, flow energy decreased, with the consequent infill by sediments that remained as a suspended load in the water column. The occurrence of abandoned channel as isolated bodies within floodplain deposits is probably related

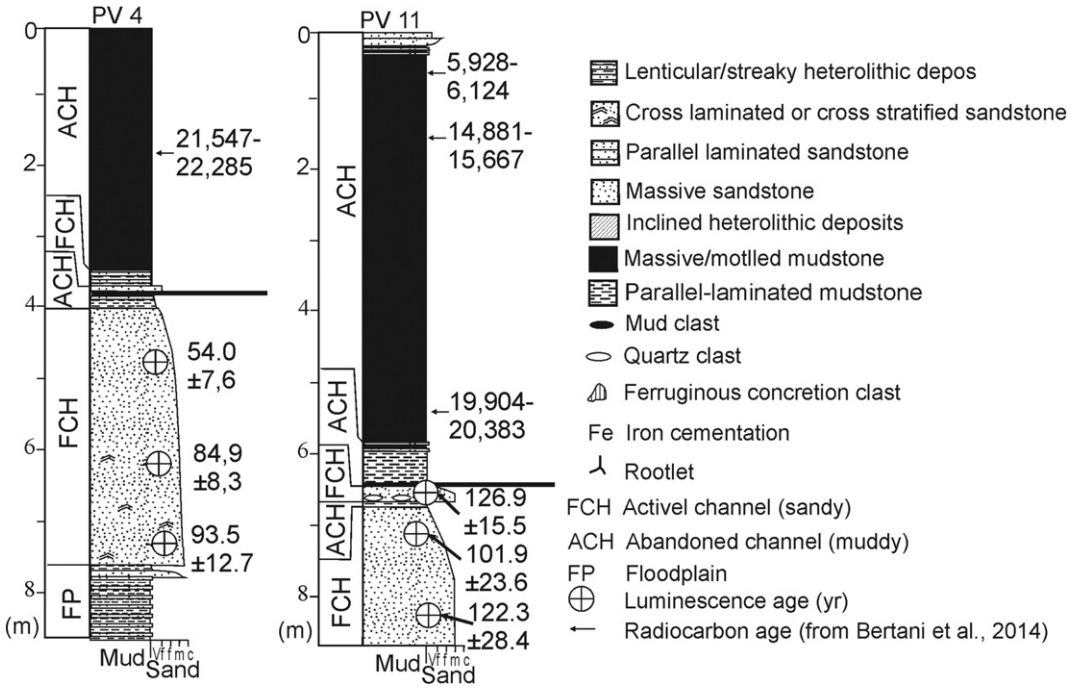

Fig. 6. Sedimentological data of the study area in the southwestern Amazonia lowland, illustrating two lithostratigraphic profiles from channels scoured down into interfluvial deposits mapped as Içá Formation (see location in Fig. 1). Note that these profiles also contain the location of OSL ages obtained in the present work, although they also includ AMS ages for the uppermost mudstones, as published in Bertani et al. (2014).

to oxbow lakes. In some instances, such as in PV4 and PV11, channel abandonment resulted in fluvial rias, as already documented in a previous publication (Bertani et al., 2014).

Mud accumulation also occurred along floodplains, and this is documented by the laterally extensive tabular packages of muddy lithologies genetically associated with channel deposits. The occurrence of parallel-laminated mudstone with heterolithic deposits in this environment, as well in the abandoned channels, records fluctuating episodes of low energy mud settling with alternating low mud settling and sand input due to momentaneous increment of water energy. The upward gradation of these lithofacies into massive pelite/mottled mudstone is common in low energy fluvial deposits, where changes in water table favor episodic subaerial exposure and soil formation. The presence of root marks and locally mud cracks in some of these strata is compatible with such interpretation. Although not exclusive, extensive floodplains are generally associated with meandering channels (e.g., Schumm, 1981).

Further evidence for channel meandering in both of the studied areas is provided by deposits related to crevasse splays. These were recognized by the lenticular nature of coarsening-upward sedimentary successions transitional into floodplain lithossomes. Crevasse splays constitute common features of meandering rivers, being formed during high water stages, when sediments transported along channels outwash their banks and reach floodplain areas (e.g., Bridge, 2003). Progradation of sandy channel sediments during such episodic high energy events produces vertically and laterally restricted, lobate-shaped sandy accumulations that spread over floodplain muds to form lenticular, coarsening-upward sand bodies (Bristow et al., 1999; Gebica and Sokolowski, 2001; Li and Bristow, in press).

Taking the interpretations provided herein into account, one can conclude that the analyzed deposits characterize fluvial depositional systems. These were pervasive over the Brazilian Amazonia, probably extending from south to north. The genetic association of active (sandy) channels with a variety of strata formed within floodplain complexes, such as oxbow lakes and crevasse splays, leads to suggest meandering fluvial systems as the most likely. Many meandering rivers have been identified in the sedimentary record by the association channel deposits with a significant volume of muddy deposits formed representative of floodplain complexes (e.g., Miall, 1996; Willis and Tang, 2010; Labrecque et al., 2011). In addition, meandering rivers usually display a considerable amount of point bars. The studied outcrops and cores did not record an expressive volume of these deposits, but the channel bars with large-scale, low-angle inclined beds may be the result of point bar migration.

7. The Içá Formation in space and time

The sedimentological and chronological data provided here lead to reexamine the geographic and temporal distributions of the Içá Formation as formerly defined in earlier times. As previously mentioned, this unit was originally related to the Plio-Pleistocene, but this age was only a rough estimate based on stratigraphic relationships. The OSL chronology presented here constitutes the first opportunity to access the depositional time of this lithostratigraphic unit based on an expressive number of absolute ages. Despite the distance between the two analyzed areas, the obtained ages for the majority of the samples approximately within the same range of variation of 65.4 ± 16.9 to 219.6 ± 25.1 ky (disregarding the three outliner ages) and 102.1 ± 9.0 to 254.8 ± 23.8 ky for deposits in southwestern and northern Amazonia, respectively, assure deposition during the Mid-Late Pleistocene. It is remarkable that all obtained ages are younger than the Plio-Pleistocene age previously estimated for fluvial deposits belonging to the Içá Formation.

The importance of such widespread young fluvial deposition along a vast area of the Amazonian lowland was recognized in a previous work (Rossetti et al., 2005), but by that time, the chronology was constrained solely by a few ^{14}C ages. The substantial amount of absolute OSL ages provided in the present work records much older ages for these fluvial deposits. These results are in agreement with a few OSL ages previously obtained for deposits of the Solimões and Negro River basins located to the west of the city of Manaus in central Amazonia (Soares et al., 2010). Although these authors recorded alluvial deposits with ages varying from 67.40 to 1.30 ky, two older ages of 427.00 ± 44 and 249.00 ± 30 ky were also documented for deposits depicted as Içá

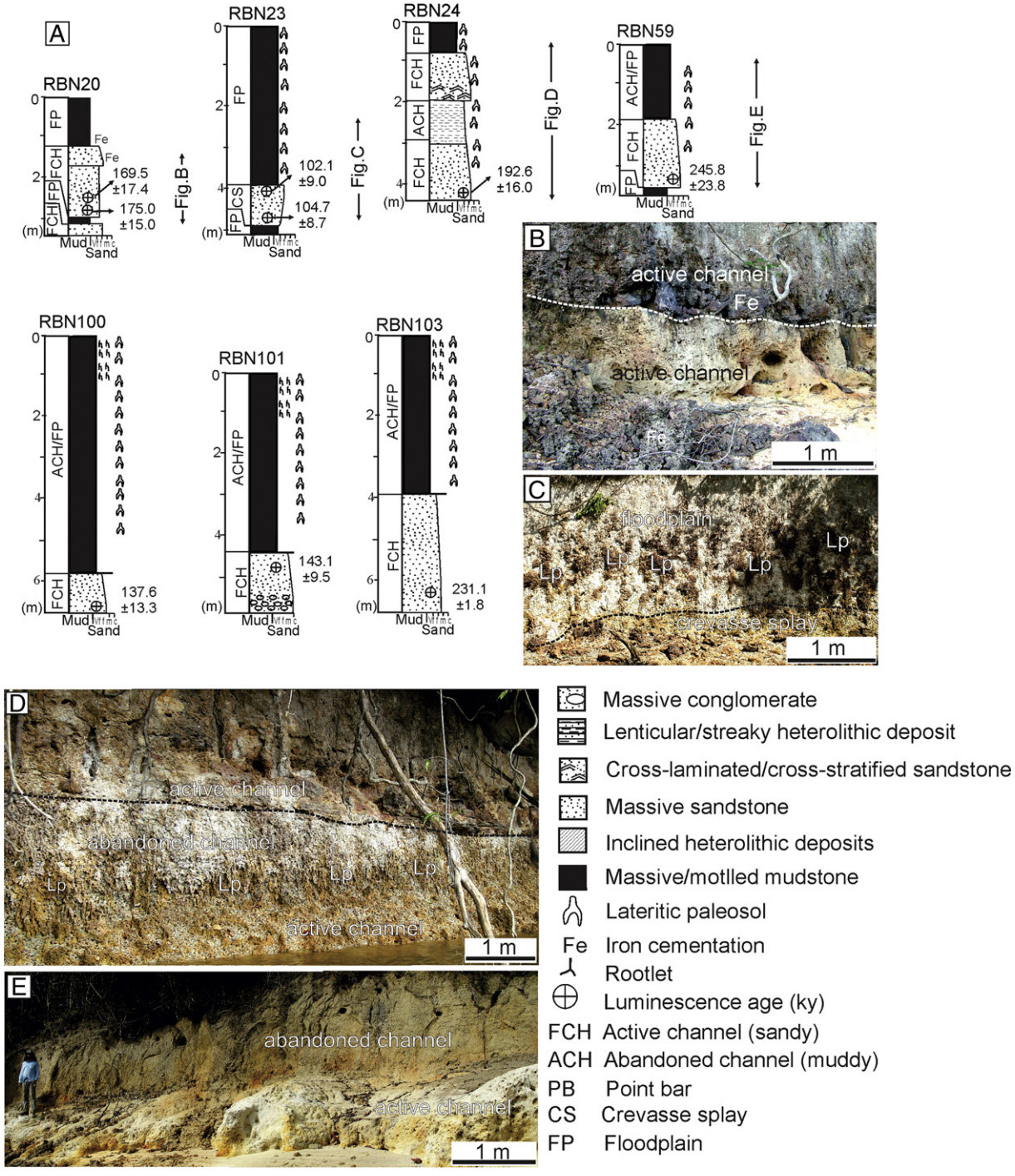

Fig. 7. Sedimentological data of the study area in northern Amazonian lowland. A) Lithostratigraphic profiles (see location in Fig. 1). B–E) View of outcrops with the spatial relationship of various deposits representative of fluvial depositional systems. See location of figures B to E in A (Fe in B = cemented sandstones; Lp in C and D = lateritic paleosol concretions).

Formation in that region. In addition, a recent work focused on pollen analysis proposed a Pleistocene age for the Içá Formation exposed further west along the Solimões River (Nogueira et al., 2013).

The Mid-Late Pleistocene ages obtained for the studied deposits lead to raise two hypotheses: 1. the meandering fluvial systems recorded by the Içá Formation throughout the Brazilian Amazonia are younger than primarily estimated; or 2. the studied deposits document a separate and extensive event of fluvial deposition that post-dates sedimentation of the Içá Formation. Both hypotheses need further investigation, particularly with additional OSL dating of samples from outcrops where this unit was originally defined, i.e., along the Içá River (see h in Fig. 1). Despite this stratigraphic problem, a key point of interest that becomes evident from the considerable set of absolute OSL ages presented here is the existence of an expressive event of sediment deposition by meandering fluvial systems over an extensive area of western Amazonia during the Mid-Late Pleistocene. In fact, considering that the ages obtained here did not reach the base of this younger fluvial succession, one should not discard the possibility that such event may have started earlier in the Pleistocene. This is also possible considering that some samples had equivalent doses near the saturation doses for quartz OSL signal using blue stimulation. For the sake of this doubt, the paleogeographic history presented below considers a generic Pleistocene age for the studied deposits. The new proposal of having widespread Pleistocene deposits over the Amazonian lowland contrasts with earlier

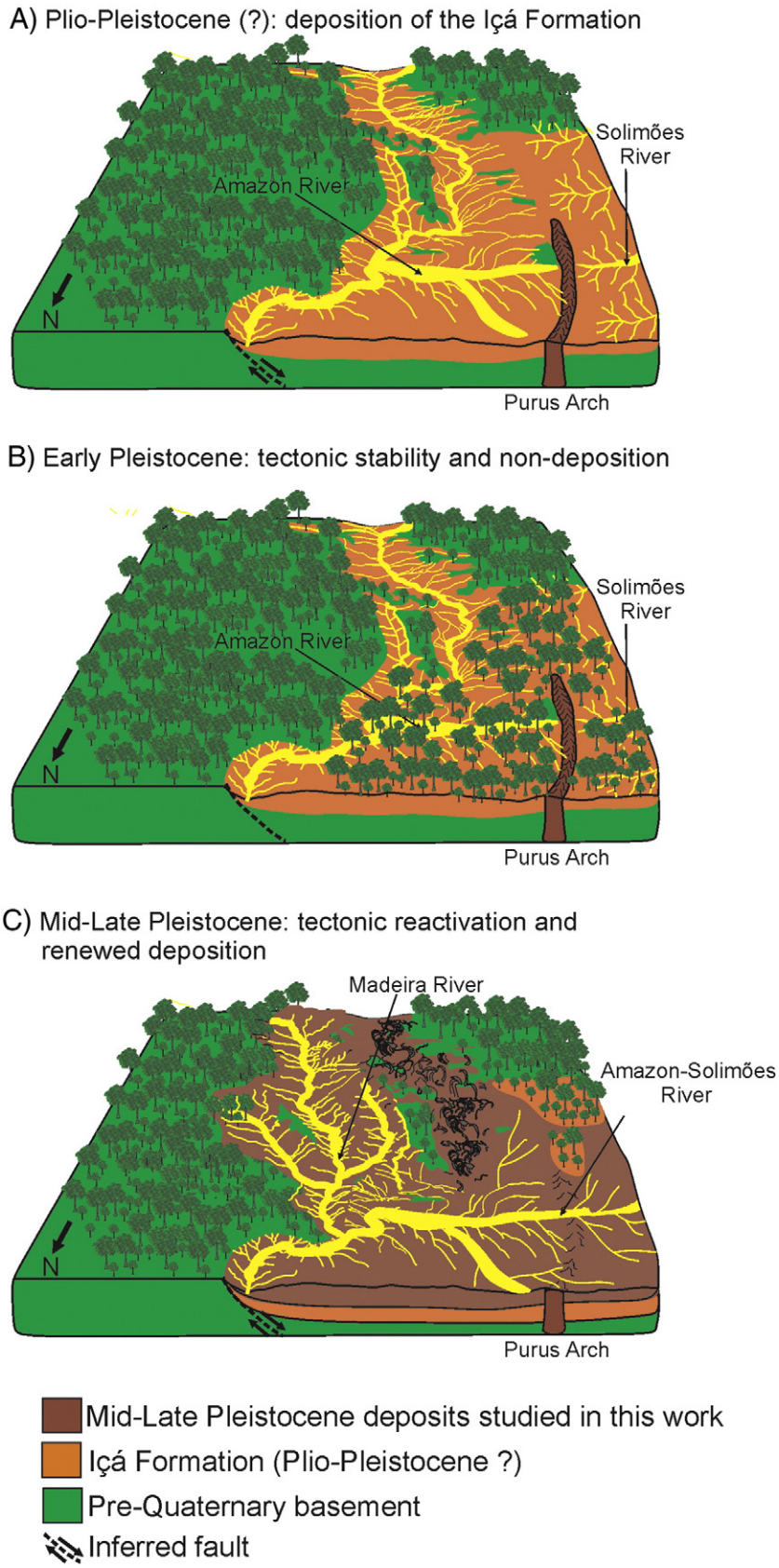

Fig. 8. Schematic model explaining the origin of the transcontinental Amazon drainage in the Mid-Late Pleistocene. A) Tectonic activity would have created space to accommodate sediments of the Içá Formation in the Plio-Pleistocene (?). During this time, the Purus arch acted as a drainage divide, separating the Amazon River to the east from drainage basins, represented by the Solimões River, to the west. B) Tectonic stability would have led to a time of erosion and non-deposition following sedimentation of the Içá Formation. The early Pleistocene time was inferred for this event with basis on the assumption that the Içá Formation was formed in the Plio-Pleistocene. C) Tectonic reactivation would have created space to accommodate new sedimentation through the Pleistocene. During this time, the Purus arch would have been eroded or subsided, a process that allowed the westward expansion of the Amazon River and its connection to western drainage basins.

views of such sedimentary record being geographically restricted to narrow terraces neighboring modern river banks. Instead, fluvial deposits of this age do occupy pervasive interfluvial areas that extend well beyond river valleys. Such situation is compatible with the maintenance of high fluvial dynamics during a period of time long enough for allowing the majority of the region to be covered by fluvial deposits.

8. Paleogeographic implication for the transcontinental Amazon pathway

It has been of overall consensus that the Amazon River reversed its course through time, changing from a primary westward flow into the Pacific Ocean to its modern configuration with the discharge eastward into the Atlantic Ocean. However, when such event occurred in the geological time is a question still open for debate. A line of evidence has been used in support of a Miocene age for the establishment of the eastward transcontinental fluvial Amazon system. For instance, a Miocene age for this event has been defended in several stratigraphic works (e.g., Damuth and Kumar, 1975; Hoorn, 1994; Hoorn et al., 1995; Gorini et al., 2013). These studies are in agreement with the proposal of an eastward expansion of the Amazon River linked to increased sedimentation rate in the Amazon fan as far back as 11.8 to 11.3 Ma (Figueiredo et al., 2009) or 10.5 Ma as corrected in Figueiredo et al. (2010). They are also in agreement with the model of mantle convection and plate kinematics proposed by Shepard et al. (2013), who established the reversal of the Amazon River as old as 14 Ma.

A few main complications concerning the Miocene age for the Amazon reversal are quoted, which include: (i) interpretations are mostly from offshore areas located >2000 km from the scenario of drainage reversal; (ii) the chronology used in these interpretations (e.g., Gorini et al., 2013; Shepard et al., 2013) are neither original, nor based on absolute ages, with the exception of the nanofossil biostratigraphy of Figueiredo et al. (2009, 2010), otherwise criticized by Campbell 2010); and (iii) linking the Amazon River reversal to the late Miocene increased sedimentation rates in the Amazon fan is ambiguous, as such event could respond to continental erosion by other existing drainage systems. Additionally, there is no sedimentary record of a transcontinental fluvial system from the mid Miocene to Pliocene in western Amazonia, which was instead dominated by Andean-derived lacustrine to fluviodeltaic deposits of the Solimões Formation (e.g., Vaz et al., 2007; Nogueira et al., 2013). The latter unit was never connected with fluvial deposits of the Novo Remanso Formation recorded eastward of the Purus Arch (Rozo et al., 2005). Contrary to the Solimões Formation, this unit had a significant source in the Amazonian cratonic areas (Nogueira et al., 2013) and also does not contain Andean palinomorphs (Dino et al., 2012).

On the other hand, the establishment of a transcontinental Amazon drainage system after the Miocene has been also defended by several other workers. For instance, Latrubesse et al. (2010) proposed that the Amazon fluvial system integrated regionally to acquire its present configuration only in the early Pliocene, although this age was postulated based on indirect correlation with events of Andean uplift. Campbell et al. (2006), also followed by Nogueira et al. (2013), established the onset of this event in the Plio-Pleistocene. However, Bezerra (2003) considered a Pleistocene–Holocene age for the establishment of many Amazonian rivers.

It follows from the foregoing discussion that determining the timing for the establishment of the Amazonian transcontinental system still requires further investigation. In this context, we postulate that the widespread distribution of fluvial deposits designated as Içá Formation over a vast area of western Amazonia must contain the sedimentary record of the Amazon expansion. A previous publication based on analyses of detrital heavy minerals combined with zircon grain U–Pb ages of Içá Formation (i.e., Horbe et al., 2013) had already raised this hypothesis. These authors recorded significant Andean sediment sources into central Amazonia only after 2.4 Ma ago, when the Iquitos arch would have subsided, allowing the connection between the Amazonas and Solimões Rivers by westward drainage expansion. Their proposal was based on the recognition of: 1. a lower Içá Formation with stable heavy minerals supplied from Mesozoic rocks of the Guiana and Brazil-Central Shields up to the Plio-Pleistocene (i.e., between 6.8 and 2.4 Ma); and 2. an upper Içá Formation having an unstable heavy mineral assemblage supplied mainly from Andean sources during the Pleistocene, i.e., after 2.4 Ma. However, these ages were postulated assuming the Plio-Pleistocene age for deposits related to the lower Içá Formation as estimated in previous publications (e.g., Maia et al., 1977). Taking this into account and also considering the hypothesis that the deposits described in the present work correspond to the Içá Formation, it follows that such paleogeographic scenario depicting the transcontinental Amazon expansion could have rather occurred sometime within the Pleistocene.

The second hypothesis presented here must be also discussed, i.e., that the studied Pleistocene deposits record a separated fluvial sedimentation after deposition of the Içá Formation (Fig. 8). Indeed, it is possible that Plio-Pleistocene deposits corresponding to the Içá Formation, as originally defined, do occur in Amazonian areas. In addition to the Içá River, these deposits can be found in numerous isolated exposures underlying Mid-Late Pleistocene deposits throughout the Solimões-Amazonas Rivers. It is interesting to note that Rossetti et al. (2005) described a sedimentary unit with a stable heavy mineral assemblage overlying the Solimões Formation along this river system, which was related to the Içá Formation. This unit is overlain by Pleistocene and Holocene units displaying an unstable heavy mineral assemblage related to Andean-sources. Such mineralogical descriptions match well with the one provided for the lower and upper Içá Formation of Horbe et al. (2013), respectively.

Therefore, we support the existence of an older (Plio-Pleistocene?) Içá Formation mapped regionally only along a narrow belt in western Amazonia and as isolated deposits underlying Mid-Late Pleistocene strata to the east. These older deposits must be distinguished from much more widespread Pleistocene and Holocene sediments, somehow as depicted in Rossetti et al. (2005). According to these authors, tectonic activity would have contributed to induce the accumulation of fluvial deposits of the Içá Formation throughout the Amazonian lowlands (Fig. 8A). After a period of tectonic quiescence, when erosion and soil formation took place, the region would have been undergone a phase of tectonic subsidence with displacement of the Içá Formation (Fig. 8B). This hypothesis is sustained by numerous data evidencing the relevance of neotectonic reactivations in the western Amazonian lowland, as summarized in a review publication (Rossetti, 2014). Such geological scenario would have created space to accommodate new sediments during the Pleistocene and formed a separated depositional unit overlying the Içá Formation throughout a vast area of western Amazonia (Fig. 8C).

If the interpretation of sediment sources for both the Içá Formation and the Pleistocene deposits is accepted, then the available information would point to the latter as the most likely candidate for having the sedimentary record corresponding to the transcontinental pathway of the Amazon River system into the Atlantic Ocean (Fig. 8C). In this instance, a paleogeographic model having the Amazonian lowland with a landscape still influenced by the Purus Arch during the Plio-Pleistocene would be more likely (Fig. 8A). Thus, a hypothesis to be considered is that this structure would have acted as a drainage divide separating the eastward flowing Amazon River from drainage systems developed to the west. Only with erosion and/or subsidence of this arch is that the Amazon River amplified westward to establish its connection with the Solimões River basin in order to transform into the longest transcontinental river on Earth as seen today.

The establishment of such relatively young drainage basin certainly had a strong effect on the Amazonian biogeography. Therefore, combining biogeographic and geological data might be valuable for better defining the timing of key events relative to the evolution of the Amazon

River. In this context, phylogenetic and biogeographic analyses by Ribas et al. (2011) led to propose the establishment of the current Amazon system at approximately 2.7 and 2 Ma. Their hypothesis considers large rivers as long-lasting barriers for some species of bird. It is noteworthy to comment, however, that these data only support the existence of a river separating sister lineages at that time. According to their model, this river was located mostly to the east of the city of Manaus, thus it did not necessarily correspond to the transcontinental Amazon River as we see today. In fact, they reconstructed that this river became connected to its main tributaries, such as the Solimões, Madeira, Negro, Tapajós, Xingu and Tocantins rivers, mostly through the Pleistocene. Such proposal is in agreement with other publications on biogeography, which indicate the formation of major Amazonian tributaries in the mid-Pleistocene, an event that would have followed rapid speciation events for several squirrel monkey taxa (Ronchail et al., 2006; Alfaro et al., 2015).

9. Conclusion

OSL dating of a considerable amount of samples derived from deposits assigned to the Içá Formation allowed recognize sedimentation only during the Mid-Late Pleistocene. This finding is important as such deposits, which contain a significant record of the evolution of the Amazon fluvial system, have been regarded as displaying an estimated Plio-Pleistocene age. The Mid-Late Pleistocene deposits record widespread development of meandering fluvial systems over a vast area of the western Amazonia lowland that extend beyond modern river valleys and occupy entire interfluvial areas. The data presented here, integrated with provenance studies available in previous publications, support a main Andean source for these fluvial sediments. Such scenario contrasts with the proposed source in cratonic areas of the Guiana and Brazil-Central shields claimed for strata of presumably Plio-Pleistocene age that underlie the studied Mid-Late Pleistocene deposits. A main paleogeographic implication that can be extracted from these data is that probably there were two important events of extensive fluvial sedimentation in the Amazonian lowland. The first event is represented by the Içá Formation and consisted of fluvial systems having their headwaters in Precambrian areas of the Amazonian craton during the Plio-Pleistocene. During this time, the Purus Arch most likely represented a central relief element on the landscape of the Amazonian lowlands, where it acted as a drainage divide and kept the Amazon River eastward. The second extensive fluvial episode occurred in the Mid-Late Pleistocene and the sedimentary successions formed during this time may contain the main record of the transcontinental Amazon pathway into the Atlantic Ocean. Such hypothesis should be better investigated with basis on further studies focusing on depositional environments, chronology and provenance from several other areas where deposits of Mid-Late Pleistocene and estimated Plio-Pleistocene ages are present. In addition, adding biogeographic data to geological information may provide more precise models to determine the timing of establishment of the Amazon drainage basin.

Acknowledgments

This work was made possible by data collected during the development of the following projects: 2010/09484-2 and 13/50475-5 (Research Funding Institute of the State of São Paulo—FAPESP) and 550331/2010-7 (Brazil's National Council for Scientific and Technological Development—CNPq). The Brazilian Geological Survey—CPRM provided transportation during field works in Rondônia and Roraima. Antonio Lisboa and Beatriz Lisboa from the ICMBio-Chico Mendes Institute for Biodiversity Conservation helped with the logistics during fieldwork in the Viruá National Park. The M.Sc. Fabio Corrêa Alves helped with part of the OSL analyses. The authors also acknowledge the logistic support provided by the Brazilian Geological Survey—CPRM and the Santo Antonio Hydroelectric during field campaigns.

References

Adamiec, G., Aitken, M.J., 1998. Dose-rate conversion factors: update. Ancient TL 16, 37–50.
Alfaro, J.W.L., Boubli, J.P., Paim, F.P., Ribas, C.C., da Silva, M.N.F., Messias, M.R., Röhe, F., Mercês, M.P., Silva Júnior, J.S., Silva, C.R., Pinho, G.M., Koshkarian, G., Nguyen, M.T.T., Harada, M.L., Rabelo, R.M., Queiroz, H.L., Alfaro, M.E., Farias, I.P., 2015. Biogeography of squirrel monkeys (genus Saimiri): south-central Amazon origin and rapid pan-Amazonian diversification of a lowland primate. Molecular Phylogenetics and Evolution 82, 436–454.
Bertani, T.C., Rossetti, D.F., Hayakawa, E.H., Cohen, M.C.L., 2014. Understanding fluvial rias based on a Late Pleistocene–Holocene analog. Earth Surface Processes and Landforms 40, 285–426.
Bezerra, P.E.L., 2003. Compartimentação Morfotectônica do Interflúvio Solimões-Negro. Univ. Fed, Pará, Belém.
Bridge, J., 2003. Rivers and floodplains: forms, processes, and sedimentary record. Blackwell Science Ltd., United Kingdom.
Bristow, C.S., Skelly, R.L., Ethridge, F.G., 1999. Crevasse splays from the rapidly aggrading, sand-bed, braided Niobrara River, Nebraska: effect of base-level rise. Sedimentology 46, 1029–1047.
Campbell, K.E., 2010. Comment on Late Miocene onset of the Amazon river and the Amazon deep-sea fan: evidence from the Foz do Amazonas Basin. Geology 38, 212.
Campbell, K.E., Frailey, C.D., Romero-Pittman, L., 2006. Ucayali Peneplain, late Neogene sedimentation in Amazonia and the birth of modern Amazon River system. Palaeogeography Palaeoclimatology Palaeoecology 239, 166–219.
Cozzuol, M., 2006. The acre vertebrate fauna: diversity, geography and time. Journal of South American Earth Sciences 21, 185–203.
CPRM, 2010. Mapa geológico do Brasil. Serv. Geol, Brasil, Brasília ([Online] URL: http://geobank.sa.cprm.gov.br (accessed December 2010)).
Damuth, J., Kumar, N., 1975. Amazon cone: morphology, sediments, age, and growth pattern. Geological Society of America Bulletin 6, 863–878.
Dino, R., Soares, E.A.A., Antonioli, L., Riccomini, C., Nogueira, A.C.R., 2012. Palynostratigraphy and sedimentary facies of Middle Miocene fluvial deposits of the Amazonas Basin, Brazil. Journal of South American Earth Sciences 34, 61–80.
Duller, G.A.T., 2004. Luminiscence dating of quaternary sediments: recent advances. Journal of Quaternary Science 19, 183–192.
Figueiredo, J., Hoorn, C., ven der Ven, P., Soares, E., 2009. Late Miocene onset of the Amazon River and the Amazon deep-sea fan: evidence from the Foz do Amazonas basin. Geology 37, 619–622.
Figueiredo, J., Hoorn, C., van der Ven, P., Soares, E., 2010. Late Miocene onset of the Amazon River and the Amazon deep-sea fan: evidence from the Foz do Amazonas Basin. Reply to comment by Campbell, K. Geology 38, 213.
Galbraith, R.F., Roberts, R.G., Laslett, G.M., Yoshida, H., Olley, J.M., 1999. Optical dating of single and multiple grains of quartz from Jinmium rock shelter, northern Australia: Part I. Experimental design and statistical models. Archaeometry 41, 339–364.
Gebica, P., Sokolowski, T., 2001. Sedimentological interpretation of crevasse splays formed during the extreme 1997 flood in the upper Vistula river valley (south Poland). Annales Societatis Geologorum Poloniae 71, 53–62.
Gorini, C., Haq, B.U., Reis, A.T., Silva, C.G., Cruz, A., 2013. Late Neogene sequence stratigraphic evolution of the Foz do Amazonas Basin, Brazil. Terra Nova 26, 179–185.
Guérin, G., Mercier, N., Adamiec, G., 2011. Dose-rate conversion factors: update. Ancient TL 29, 5–8.
Harris, S., Mix, A., 2002. Climate and tectonic influences on continental erosion of tropical South America, 0–13 Ma. Geology 30, 447–450.
Hoorn, C., 1994. An environmental reconstruction of the palaeo-Amazon River system (middle to late Miocene, NW Amazonia). Palaeogeography Palaeoclimatology Palaeoecology 112, 187–238.
Hoorn, C., Guerrero, J., Sarmiento, G.A., Lorente, M.A., 1995. Andean tectonics as a cause for changing drainage patterns in Miocene northern South America. Geology 23, 237–240.
Horbe, A.M.C., Motta, M.B., Almeida, C.M., Dantas, E.D., Vieira, L.C., 2013. Provenance of Pliocene and recent sedimentary deposits in western Amazônia, Brazil: consequences for the paleodrainage of the Solimões-Amazonas River. Sedimentary Geology 296, 9–20.
INPE, 2010. Studies from INPE indicate that the Amazon River is 140 km longer than the Nile. Brazilian Nat. Inst. Space Res (Retrieved 3 August 2010).
Labrecque, P.A., Hubbard, S.M., Jensen, J.L., Nielsen, H., 2011. Sedimentology and stratigraphic architecture of a point bar deposit, Lower Cretaceous McMurray formation, Alberta, Canadá. Canadian of Petroleum Geologists Bulletin 59, 147–171.
Latrubesse, E.M., 2008. Patterns of anabranching channels: the ultimate end-member adjustment of mega rivers. Geomorphology 101, 130–145.
Latrubesse, E.M., Ramonell, C., 1994. A climatic model for southwestern Amazonia at Last Glacial times. Quaternary International 21, 163–169.
Latrubesse, E., Cozzuol, M., Caminha, S.S., Rigsby, C., Absy, M., Jaramillo, C., 2010. The Late Miocene paleogeography of the Amazon Basin and the evolution of the Amazon River system. Earth Science Reviews 99, 99–124.
Li, J., Bristow, C.S., 2015. Crevasse splay morphodynamics in a dryland river terminus: Río Colorado in Salar de Uyuni Bolivia. Quaternary International 377, 71–82.
Maia, R.G., Godoy, H.K., Yamaguti, H.S., Moura, P.A., Costa, F.S., 1977. Projeto carvão no Alto Amazonas. Final report. CPRM, Rio de Janeiro.

McLaurin, B.T., Steel, R.J., 2007. Architecture and origin of an amalgamated fluvial sheet sand, lower Castlegate Formation, Book Cliffs, Utah. Sedimentary Geology 197, 291–311.
Miall, A.D., 1996. The geology of fluvial deposits: sedimentary facies, basin analysis, and petroleum geology. Springer-Verlag, Berlin Heildelberg (582 pp.).
Mora, A., Baby, P., Roddaz, M., Parra, M., Brusset, S., Hermoza, W., Espurt, N., 2010. Tectonic history of the Andes and Sub-Andean zones: implications for the development of the Amazon Drainage basin. In: Hoorn, C., Wesselingh, F.P. (Eds.), Amazonia: Landscape and Species Evolution, a Look into the Past. Wiley Online Library, pp. 38–60.
Murray, A.S., Wintle, A.G., 2003. The single aliquot regeneration dose protocol: potential for improvements in reliability. Radiation Measurements 37, 377–381.
Nogueira, A.C.R., Silveira, R., Guimarães, J.T., 2013. Neogene Quaternary sedimentary and paleovegetation history of the eastern Solimões Basin, central Amazon region. Journal of South American Earth Sciences 46, 89–99.
Prescott, J.R., Stephan, L.G., 1982. The contribution of cosmic radiation to the environmental dose for thermoluminescence dating: latitude, altitude and depth dependencies. Journal Council Europe PACT 6, 17–25.
Radambrasil, 1978. Folha SB.20 Purus-Geologia 17. Dep. Nac. Prod. Min.-DNPM, Rio de Janeiro, pp. 19–128.
Reis, N.J., Almeida, M.E., Riker, S.L., Ferreira, A.L., 2006. Geologia e recursos minerais do Estado do Amazonas (texto explicativo dos mapas geológicos e de recursos minerais do Estado do Amazonas). Serv. Geol. Brasil-CPRM, Manaus.
Ribas, C.C., Aleixo, A., Nogueira, A.C.R., Miyaki, C.Y., Cracraft, J., 2011. A palaeobiogeographic model for biotic diversification within Amazonia over the past three million years. Proceedings of the Royal Society B: Biological Sciences 279, 681–689.
Ronchail, J., Guyot, J.L., Villar, J.C.E., Fraizy, P., Cochonneau, G., Oliveira, E., Filizola, N., Ordenez, J.J., 2006. Impact of the Amazon tributaries on major floods at Obidos. Climate variability and change: hydrological impactsProc. Fifth FRIEND World Conf. 308. IAHS Pub, Havana, Cuba, pp. 220–225.
Rossetti, D.F., 2014. The role of tectonics in the late Quaternary evolution of Brazil's Amazonian landascape. Earth Science Reviews 139, 362–389.
Rossetti, D.F., Toledo, P.M., Góes, A.M., 2005. New geological framework for Western Amazonia (Brazil) and implications for biogeography and evolution. Quaternary Research 63, 78–89.
Rossetti, D.F., Zani, H., Cohen, M.C.L., Cremon, É.H., 2012. A Late Pleistocene–Holocene wetland megafan in Brazilian Amazonia. Sedimentary Geology 282, 276–293.
Rossetti, D.F., Zani, H., Cremon, É.H., 2014a. Fossil megafans evidenced by remote sensing in the Amazonian wetlands. Zeitschrift für Geomorphologie 58, 145–161.
Rossetti, D.F., Cohen, M.C.L., Bertani, T.C., Hayakawa, E.H., Paz, J.D.S., Castro, D.F., Friaes, Y., 2014b. Late Quaternary fluvial terrace evolution in the main southern Amazonian tributary. Catena 116, 19–37.
Rozo, M.G., Nogueira, A.C.R., Horbe, A.M.C., 2005. Depósitos neógenos da Bacia do Amazonas. In: Reis, J., Monteiro, M.A.S. (Eds.), Contribuições à Geologia da Amazônia. Soc. Bras. Geol 4, pp. 116–123.
Santos, O., Nelson, B., Giovannini, C.A., 1993. Corpos de areia sob leitos abandonados de grandes rios. Ciencias Hoje 16, 22–25.
Schumm, S.A., 1981. Evolution and response of the fluvial system: sedimentologic implications. Soc. Sedim. Geol. (SEPM) Spec. Publ. 31 pp. 19–29.
Shepard, G.E., Müller, R.D., Liu, L., Gurnis, M., 2010. Miocene drainage reversal of the Amazon River driven by plate–mantle interaction. Nature Geoscience 3, 870–875.
Shepard, G.E., Müller, R.D., Liu, L., Gurnis, M., 2013. Miocene drainage reversal of the Amazon River driven by plate–mantle interaction. Nature Geoscience 3, 870–875.
Soares, E.A.A., Tatumi, S.H., Riccomini, C., 2010. OSL age determinations of Pleistocene fluvial deposits in Central Amazonia. Anais da Academia Brasileira de Ciências 82, 691–699.
Sterling, T., 1979. Der Amazonas. Time-Life Bücher. 8th German Printing, p. 20.
Tassinari, C.C.G., Macambira, M.J.B., 1999. Geochronological provinces of the Amazonian Craton. Episodes 22, 174–182.
Vaz, P.T., Wanderley-Filho, J.R., Bueno, G.V., 2007. Bacia do Takutu. Boletin Geociências Petrobrás 15, 289–297.
Wesslingh, F.P., Räsänen, M.E., Irion, G., Vonhof, H.B., Kaandorp, R., Renema, W., Romero-Pittman, L., Gingras, M., 2001. Lake Pebas: a palaeoecological reconstruction of a Miocene long-lived lake complex in Western Amazonia. Cainozoic Research 1, 35–81.
Willis, B.J., Tang, H., 2010. Three-dimensional connectivity of point-bar deposits. Journal of Sedimentary Research 80, 440–454.